The 2025 World Congress on
Advances in Structural Engineering and Mechanics (ASEM25)
BEXCO, Busan, Korea, August 11-14, 2025

Reliability-based calibration of axial and shear strength models for composite walls in AS/NZS 2327

Won-Hee Kang[1)], Mahbub Khan[2)], Jun Mo[3)], Youtian Wang[4)] Brian Uy[5)] and Huu-Tai Thai*[6)]

[1)] *School of Engineering, Design & Built Environment, Western Sydney University, Penrith 2751, Australia*

[2), 5)] *School of Civil and Environmental Engineering, The University of New South Wales, Kensington, NSW 2052, Australia*

[3)] *School of Civil Engineering, The University of Sydney, Sydney, NSW 2006, Australia*

[4)] *Department of Building and Real Estate, Hong Kong Special Administrative Region of China, The Hong Kong Polytechnic University, PR China*

[6)] *Department of Infrastructure Engineering, The University of Melbourne, Parkville, VIC 3010, Australia*

[6)] *tai.thai@unimelb.edu.au*

ABSTRACT

Composite walls are widely used in mid- and high-rise buildings for their structural efficiency and performance. To support reliable structural design, this study focuses on the accurate and cost-safety balanced estimation of axial and shear strength. It presents a structural reliability-based calibration of capacity factors for composite walls, contributing to the development of new design provisions in AS/NZS 2327. A total of 64 axial compression and 23 shear test results were collected from existing literature to evaluate and calibrate the design equations. Axial strength was predicted using a model based on effective length and concrete contribution factors, while in-plane shear strength was estimated using a simplified mechanics-based model. The reliability-based calibration procedure follows the methodology outlined in AS 5104, ISO 2394 and Eurocode 0 Annex D, aligning with recent practices in structural design standards calibrations. Capacity factors were determined using the first-order reliability method sensitivity factor concept, under consistent assumptions on uncertainty distributions and target reliability indices, as applied in similar practices, for example in the calibration of composite columns. Separate capacity factors for steel and concrete components were

---

[1)] Associate Professor
[2)] Senior Research Associate
[3)] Former PhD student
[4)] Postdoctoral Fellow
[5)] Scientia Professor
[6)] Professor

derived to account for material-specific behaviour, and also a unified factor format was adopted to minimise modelling uncertainty. The calibration shows that, for axial compression, a unified capacity factor of 0.64–0.89 meets the target reliability for varying concrete reduction factors, with a recommended value of 0.70 when a concrete strength reduction factor of 0.85 is applied; fixing the steel factor at 0.90 yields concrete factors of 0.50–0.83. For in-plane shear, a single unified factor of 0.77 is obtained. These findings provide a statistically consistent basis for the proposed AS/NZS 2327 design provisions for composite walls.

1. INTRODUCTION

Concrete-filled steel plate composite walls are increasingly adopted in tall buildings and critical infrastructure due to their considerable structural capacity and construction efficiency. These systems consist of two exterior steel plates connected by shear connectors and filled with concrete, creating composite action that enhances both axial and shear resistance while mitigating local buckling. The modular design of such composite walls enables fast assembly, supporting the construction of tall buildings and structures requiring seismic resilience (Mo et al. 2022; Broberg et al. 2022). The steel plates serve as both permanent formwork and reinforcement, while the confined concrete core enhances lateral stability and helps resist inward buckling of the plates. This composite behaviour improves strength, energy dissipation, and seismic capacity, contributing to overall structural resilience and safety (Mo et al. 2022).

As the use of these wall systems continues to grow, it becomes increasingly important to transform predictive strength models into practical design models for structural engineering applications. Accurate estimation of axial compressive strength and appropriate calibration of capacity factors are also necessary to improve a cost-effective and safe design. Important variables affecting capacity include local buckling in slender faceplates, the interaction between concrete and steel, and the level of shear connection. The faceplate slenderness, often defined by the stud spacing-to-thickness ratio, is critical in determining the failure mechanism, either yielding or buckling. Material properties such as steel yield strength and concrete compressive strength also influence structural response (Zhang et al. 2020). The prediction model considered in this study was developed based on empirical formulations and semi-empirical approaches, supported by large-scale tests and comprehensive data analysis (Mo 2022).

The in-plane shear behaviour of concrete-filled steel plate composite walls is also significant, particularly under seismic or blast loading conditions. This study adopts a simplified shear design equation derived from AISC (2015) and the work of Varma et al. (2013). Seo et al. (2016) further examined alternative equations and investigated how parameters such as the reinforcement ratio in steel faceplates, support conditions, and core thickness influence failure modes like anchorage failure or yielding. For consistency in practical engineering applications, the simplified model is adopted as the primary design method in this study, while other models are referenced to enhance understanding of shear performance under complex loads.

Achieving the required reliability level in structural design using these models needs the application of statistical and probabilistic methods to evaluate appropriate safety margins. This includes the calibration of capacity factors by accounting for uncertainties in design inputs, modelling assumptions, and limited data availability. Previous simplified reliability studies by Zhang et al. (2020) and Seo et al. (2016) assumed normal distributions for capacities. Building on these, this study calibrates capacity factors for the AS/NZS 2327 design code using reliability-based methods aligned with AS 5104, ISO 2394, and Eurocode 0 Annex D. Based on an extensive experimental dataset, this study contributes to the development of accurate and reliable design models for composite walls, supporting new design provisions in AS/NZS 2327 (Standards Australia/Standards New Zealand 2017).

2. RELIABILITY BASED CAPACITY FACTOR CALIBRATION

2.1 Target reliability index

Capacity factors are calibrated to meet the consequence level of failure in structural design, defined by a target reliability index. The relationship between the failure probability P_f and the reliability index β is defined as follows:

$$P_f = \Phi(-\beta) \tag{1}$$

where Φ = the cumulative distribution function (CDF) of the standard normal distribution.

AS 5104 (Standards Australia 2017) and ISO 2394 (International Organization for Standardization 1998) recommend a target reliability index of β_1 = 4.4 for the ultimate limit state (ULS), corresponding to a one-year reference period, in cases where the consequences of failure are significant and the relative cost of safety measures is moderate. Most international design standards determine capacity reduction factors based on a 50-year reference period, and, the previous version of ISO 2394 (International Organization for Standardization 1998) and EN 1990 (CEN 1990) prescribe a target reliability index of β_{50} = 3.8. As specified in EN 1990, the reliability index for different reference periods can be derived using the following equation:

$$\Phi(\beta_n) = [\Phi(\beta_1)]^n \tag{2}$$

where β_n denotes the reliability index corresponding to an n-year reference period, and β_1 is the reliability index associated with a one-year reference period.

By applying Eq. (2), it follows that a reliability index of β_{50} = 3.8 corresponds to β_1 = 4.7 under the assumption of full statistical independence of failure events across years. However, this assumption is not realistic, and a more reasonable interpretation, as suggested in ISO2394:1998 (International Organization for Standardization 1998), is that β_{50} = *3.8* is approximately equivalent to β_1 = *4.4*. Based on this interpretation and to align with the approach adopted in international design standards for steel and composite structures, this study adopts a target reliability index of $\beta_t = \beta_{50}$ = 3.8, based on a 50-year reference period.

In scenarios where resistance alone is considered disregarding the load effect, the associated probability is related to its reliability index by the following expression:

$$P(R \leq R_d) = \Phi(-\alpha_d \beta_t) = \Phi(-\beta_R) \tag{3}$$

where α_d is the sensitivity factor used in the First-Order Reliability Method (FORM) (CEN 1990), with a recommended value of 0.8 as specified in AS 5104 (Standards Australia 2017) and ISO 2394 (International Organization for Standardization 1998), R denotes the resistance, and R_d represents the design resistance.

2.2 Capacity factor calibration procedure

The capacity factor calibration approach adopted in Kang et al. (2018, 2021), based on EN 1990 Annex D.8 (CEN 1990), is used for reliability analysis while accounting for parametric, modelling, and statistical uncertainties. This method assumes the resistance variable is non-negative consistent with physical reality, and models this using a lognormal distribution. The calibration procedure separates capacity factors from load factors by applying the First-Order Reliability Method (FORM) (Der Kiureghian 2005), in which a sensitivity factor (α) is used to distinguish the contributions of resistance and load in the reliability assessment.

In this framework, the modelling uncertainty is quantified statistically by comparing predicted resistance values from the model with corresponding experimental results. The capacity factor (ϕ) associated with a given resistance prediction model is defined as follows:

$$\phi = \frac{R_d}{R_n} \tag{4}$$

where R_d denotes the design resistance required to satisfy the target reliability level for resistance, and R_n denotes the nominal or characteristic resistance.

To evaluate these parameters, first assume that $g_R(\boldsymbol{x})$ is a resistance prediction model, where $\boldsymbol{x}$ is a vector comprising the mean-measured values of the design parameters. The constant bias in this model can be statistically expressed as:

$$\bar{b} = \frac{1}{N}\sum_{i=1}^{N}\left(\frac{R_{ei}}{R_{ti}}\right) \tag{5}$$

where N is the total number of experimental data, R_{ei} is the measured resistance of the i^{th} specimen, and R_{ti} is the corresponding resistance predicted by the resistance model $g_R(\boldsymbol{x}_i)$ for the i^{th} specimen. Including the bias correction factor, the unbiased resistance prediction R is calculated as follows:

$$R = \bar{b} g_R(\boldsymbol{x}) \delta \tag{6}$$

where δ = the modelling error of unbiased resistance prediction. The modelling error of the i^{th} specimen, δ_i, is calculated as follows:

$$\delta_i = \frac{R_{ei}}{\bar{b} R_{ti}} \tag{7}$$

The resistance R in Eq. (6) is assumed to follow a lognormal distribution with non-negative values, and the coefficient of variation (COV) of the resistance (R) is estimated using

the following equation:

$$V_R \cong \sqrt{V_\delta^2 + V_{Rt}^2} \tag{8}$$

where V_δ = the COV of the modelling error, estimated from Eq. (7), and V_{Rt} = COV of the parametric uncertainty. This formulation assumes that the modelling error and parametric uncertainty are statistically independent. The value of V_{Rt} can be calculated using the Monte Carlo simulation or the first-order approximation method. The standard deviation of the logarithm of resistance, σ_{lnR}, is then estimated as follows:

$$\sigma_{lnR} = \sqrt{\ln(1 + V_R^2)} \tag{9}$$

which is used when calculating the design resistance (R_d) in Eq. (4) as follows:

$$R_d = \bar{b} g_R(\boldsymbol{x}) \exp\left(-k\sigma_{lnR} - 0.5\sigma_{lnR}^2\right) \tag{10}$$

where

$$k = \frac{k_{d,m} V_\delta^2 + \beta_R V_{Rt}^2}{V_R^2} \tag{11}$$

where $k_{d,m}$ is the fractile factor corresponding to a finite number of structural member tests, to consider the statistical uncertainty from limited test sample sizes. The fractile factor is defined for a target reliability index for resistance (β_R) at a 75% confidence level and can be estimated for an unknown σ_{lnR} through the following expression:

$$k_{d,m} = t_\beta(n-1) \times \left(1 + \frac{1}{n}\right)^{0.5} \tag{12}$$

where t_β is the fractile of the t-distribution corresponding to the probability level defined by the target reliability index β_R.

The nominal resistance R_n in Eq. (4) is obtained from the resistance prediction model $g_R(\boldsymbol{x}_n)$ using nominal input parameters $\boldsymbol{x}_n$. If nominal values are not available, characteristic values on the 5% fractile may be used instead, or nominal parameters may be inferred from specified tolerance limits in the relevant product standards (Kang et al. 2018).

When multiple capacity factors are involved in the structural design model, and one of them needs to be evaluated while the others are held constant at specified values, the following equation can be solved using optimisation algorithms such as the Active-Set optimisation algorithm (Nocedal and Wright 2006) or pattern search (Audet and Dennis 2002):

$$R_d = g_R(\boldsymbol{x}_n; \phi_1, \ldots \phi_m; \phi_{unknown}) \tag{13}$$

where $\phi_1, \ldots \phi_m$ are capacity factors with fixed values, and $\phi_{unknown}$ is the capacity factor to be evaluated.

3. RESULTS AND DISCUSSIONS

The capacity factor calibration is conducted for two failure modes, axial compression and shear. The corresponding prediction models and the resulting calibrated capacity factors are presented in this section.

3.1 Composite walls under axial compression

The data has been collected, comprising 64 specimens of composite walls under axial compression. The database was established based on the following references: Akiyama et al. (1991), Usami et al. (1995), Kanchi et al. (1996), Choi and Han (2009), Choi et al. (2014), Yang et al. (2016), Zhang et al. (2020), and Mo (2022). This database is used to estimate the modelling error in Eq. (7) during the capacity factor calibration. The input parameters and experimental capacities are presented in Table 1.

Table 1. Composite wall database under axial compression

Reference	Specimen	f'_c (MPa)	f_y (MPa)	b (mm)	t_w (mm)	t_s (mm)	s/t_s	P_{test} (KN)
Akiyama et al. (1991)	NS50	23	299	960	250	3.2	50	7257
	NS75	23	299	960	250	3.2	75	7012
	NS100	23	299	960	250	3.2	100	7365
Usami et al. (1995)	NS20	31	287	640	200	3.25	20	5730
	NS30	31	287	640	200	3.25	30	5470
	NS40	31	287	640	200	3.25	40	5000
	NS50	31	287	640	200	3.25	50	5050
Kanchi et al. (1996)	20M	36	353	1000	280	4.5	20	15387
	25M	36	363	1000	280	4.5	25	14877
	30M	36	358	1000	280	4.5	30	14132
	50M	36	348	1000	280	4.5	50	13827
	30S	28	321	1000	280	4.5	30	10464
	C6-20M	38	396	1000	280	6	20	17152
	C6-25M	38	396	1000	280	6	25	16769
	C6-30M	38	396	1000	280	6	30	15592
	C6-35M	38	396	1000	280	6	35	13916
	C6-30S	28	329	1000	280	6	30	11317
Choi and Han (2009)	SS400-S	42	274	380	300	6	25	6282
	SS400-M	42	274	480	300	6	33	7051
	SS400-L	42	274	680	300	6	50	8956
	SM490-S	42	418	380	300	6	25	6562
	SM490-M	42	418	480	300	6	33	8069
	SM490-L	42	418	680	300	6	50	8850
Choi et al. (2014)	C24/B20	24	428	280	250	6	20	3052
	C24/B30	24	428	370	250	6	30	3528
	C24/B40	24	428	460	250	6	40	4164
	H16/B20	16	428	280	250	6	20	2539
	H16/B30	16	428	370	250	6	30	3055

	H16/B40	16	428	460	250	6	40	3812
Yang et al. (2016)	DSC4-150	43.3	409.5	1240	240	4	37.5	11249
	DSC4-200	35.9	409.5	1240	240	4	50	10318
	DSC4-250	42.2	409.5	1240	240	4	62.5	11230
	DSC4-300	39.6	409.5	1240	240	4	75	11610
	DSC6-240	42.5	348.4	1240	240	6	40	13525
	DSC6-300	37.1	348.4	1240	240	6	50	11606
	DSC6-360	39.1	348.4	1240	240	6	60	13033
Zhang et al. (2020)	TS1-0.6	17	274	279.4	139.7	4.7	14.9	1257
	TS1-0.8	17	274	276.2	137.2	4.7	19.6	1123
	TS1-1.2	17	274	279.4	152.4	4.7	29.7	1346
	TS1-1.4	17	274	323.9	146.1	4.7	34.4	1335
	TS1-1.6	17	274	368.3	146.1	4.7	39.2	1173
	TS2-0.6	30	259	330.2	168.6	4.9	16.9	2258
	TS2-0.8	30	259	330.2	168.6	4.9	22.7	2270
	TS2-1	31	259	330.2	168.6	4.9	27.9	2304
	TS2-1.2	31	259	330.2	168.6	4.9	33.7	2089
Mo (2022)	N-CP-35	28	285	210	150	3	35	1274
	N-CP-25	28	285	150	150	3	25	1076
	H-CP-35	28	770	350	150	5	35	2840
	H-CP-25	28	770	250	150	5	25	2526
	UH-CP-35	28	1030	350	150	5	35	2850
	UH-CP-25	28	1030	250	150	5	25	2575
	N-CW-40-QS	28	285	400	140	3	40	2015
	N-CW-40-QB	28	285	400	140	3	40	1980
	N-CW-20-TS	28	285	400	140	3	20	2040
	N-CW-32-QS	28	770	400	140	5	32	3170
	N-CW-32-QB	28	770	400	140	5	32	3020
	N-CW-19.2-QS	28	770	400	140	5	19.2	3605
	N-CW-19.2-QB	28	770	400	140	5	19.2	4067
	N-CW-16-TS	28	770	400	140	5	16	3574
	N-CW-12-QS	28	770	400	140	5	12	3810
	N-CW-9.6-TS	28	770	400	140	5	9.6	3581
	UH-CW-32-QS	28	1030	400	140	5	32	3233
	UH-CW-32-QB	28	1030	400	140	5	32	3050
	UH-CW-16-TS	28	1030	400	140	5	16	3625

In this table, f'_c= characteristic compressive strength of concrete at 28 days; f_y = the yield strength of the steel plate; b: the width of the composite walls; t_w: the thickness of the composite walls; t_s = the thickness of the steel faceplate; s: the spacing of connectors in the composite walls; P_{test} = the measured axial strength of composite walls.

The section compression resistance model used in the analysis is based on a design method for composite walls, accounting for the composite action between the elements forming

the cross-section. It applies to walls with symmetrical steel plates fabricated from steel with a maximum yield stress of 690 MPa. The section compression resistance of a concentrically loaded rectangular composite wall member is calculated as follows:

$$Ns_{,Rd} = \phi(0.85A_c f'_c + A_r f_{sy} + A_s f_{cr}) \tag{14}$$

where ϕ = the unified capacity factor for walls in compression to be calibrated; A_c = cross-sectional area of concrete; A_r = cross-sectional area of reinforcement; A_s = cross-sectional area of steel plate; f_{sy}= yield strength of reinforcement. Two capacity factors can also be applied separately to the concrete and steel materials in this equation.

$$\begin{aligned} f_{cr} &= \frac{\pi^2 E}{12 \times K^2 \times (\frac{s}{t_p})^2} \leq f_y \\ &= \begin{cases} f_y, & s/t_p < \sqrt{\frac{\pi^2}{12K^2}} \times \sqrt{E/f_y} \\ \frac{\pi^2 E}{12 \times K^2 \times (\frac{s}{t_p})^2}, & s/t_p \geq \sqrt{\frac{\pi^2}{12K^2}} \times \sqrt{E/f_y} \end{cases} \end{aligned} \tag{15}$$

where E = elastic modulus of steel; K=0.7; s = longitudinal distance between studs parallel to the applied axial force; t_p = steel plate thickness.

In the reliability analysis, the random variables used for the parametric uncertainty estimation are defined as follows: the mean of each random variable is based on the mean-measured values, and their COVs are defined as follows: Yield strength of steel (f_y) has 7% COV (JCSS 2001); Compressive strength of concrete (f'_c) has 10% COV (Standards Australia 2009, Standards New Zealand 2003); steel plate thickness (t_p) has 10% COV (Standards Australia/Standards New Zealand 2009), which is a conservative assumption from the manufacturing tolerances such as Standards Australia/Standards New Zealand (2016); all other linear dimensions 1% COV Standards Australia 2004, Standards Australia/Standards New Zealand 2009).

Reliability based calibration has been conducted to find out the capacity factor to meet the target reliability index (β_t) of 3.04 for the resistance consideration only separate from the load effect, to be consistent with the calibrations for other types of structural members such as composite columns (Standards Australia/Standards New Zealand 2017).

In this analysis, strength reduction has been considered for the concrete compressive strength, similar to the approach used in the design of pure concrete walls. A range of reduction factors between 0.60 and 1.00 has been applied to account for this effect. The capacity factor has been calibrated accordingly by reflecting the influence of this strength reduction.

The capacity factor has been calculated in two different formats. The first approach uses a single unified capacity factor to the entire equation. The second approach involves using two separate capacity factors to account for the contributions of steel and concrete individually. The

use of a single unified capacity factor is beneficial because it maintains the original form of the equation, preserving the optimised or fitted prediction accuracy based on either mechanical representation or best-fit data. This approach avoids introducing additional modelling uncertainty (Kang et al. 2015). On the other hand, using separate capacity factors is advantageous for two reasons: first, it allows for a fair consideration of the different uncertainties associated with each material; second, when one material is predominantly used, it allows the strength prediction of the composite member to trend towards the strength of that dominant material.

The capacity factor calibration results are presented in Table 2. In the case of the second approach, when the steel capacity factor is fixed at 0.9, the concrete capacity factor varies between 0.83 and 0.50. This variation corresponds to an additional concrete strength reduction factor ranging between 0.60 and 1.00. For the first approach, the result can be represented as a single unified capacity factor, which ranges from 0.64 to 0.89.

The additional concrete strength reduction factor of 0.60 corresponds to a pure concrete wall, while a factor of 1.00 represents a CFST column. The capacity factors between these two cases illustrate the behaviour of composite walls that exhibit characteristics between full confinement, as in CFST columns, and no confinement, as in pure concrete walls. For structural design purposes, the recommended values are a unified capacity factor of 0.70, in conjunction with an additional concrete strength reduction factor of 0.85.

Table 2. Capacity factors calibrated for composite walls under axial compression for β_t = 3.04

Strength reduction to f'_c	The unified capacity factor	Two capacity factors (when ϕ_s is fixed as 0.90)
1.00	ϕ = 0.64	ϕ_s = 0.90 and ϕ_c = 0.50
0.85	ϕ = 0.71	ϕ_s = 0.90 and ϕ_c = 0.59
0.80	ϕ = 0.73	ϕ_s = 0.90 and ϕ_c = 0.62
0.60	ϕ = 0.89	ϕ_s = 0.90 and ϕ_c = 0.83

where ϕ_s = capacity factor for steel; ϕ_c = capacity factor for concrete.

Fig. 1 (a) presents the unified capacity factor as a function of the target reliability index, varying from 2.5 to 4.2, when there is no concrete strength reduction. The results demonstrate a decreasing trend, where the capacity factor reduces with increasing target reliability index. This relationship reflects the requirement for more conservative design as the level of reliability required increases. The figure also identifies the intersection point between the capacity factor curve and the target reliability index of 3.04. This point represents the calibrated capacity factor that meets the required level of reliability and complies with structural safety criteria, while accounting for uncertainties in the model and parameters.

As greater reductions are applied to the concrete material strength, such as 0.85, 0.80, and 0.60, as shown in Figs. 1(b)–(d), the overall capacity factor increases. The decreasing trend with respect to increasing target reliability indices remains consistent with the previous calculation, and this consistent pattern is observed across all the figures.

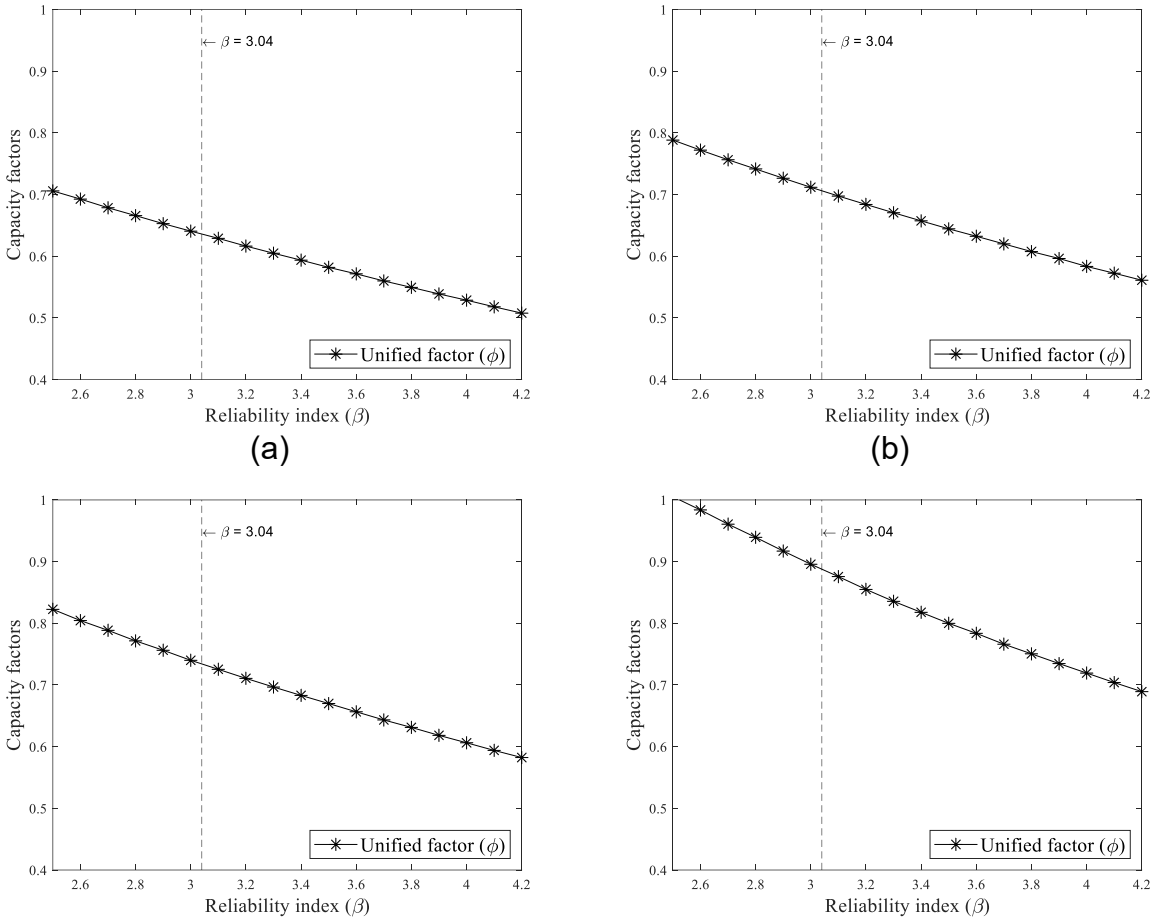

Fig. 1 Calibration for the unified capacity factor for axial compression, with the concrete strength reduction of (a) 1.00, (b) 0.85, (c) 0.80, and (d) 0.60

Fig. 2 presents the concrete capacity factor as a function of the target reliability index, with the steel capacity factor fixed at 0.9. The target reliability indices range from 2.5 to 4.2. The concrete capacity factor decreases as the target reliability index increases. Conversely, it increases as greater strength reduction is applied to the concrete material. This format can also be used for structural design purposes.

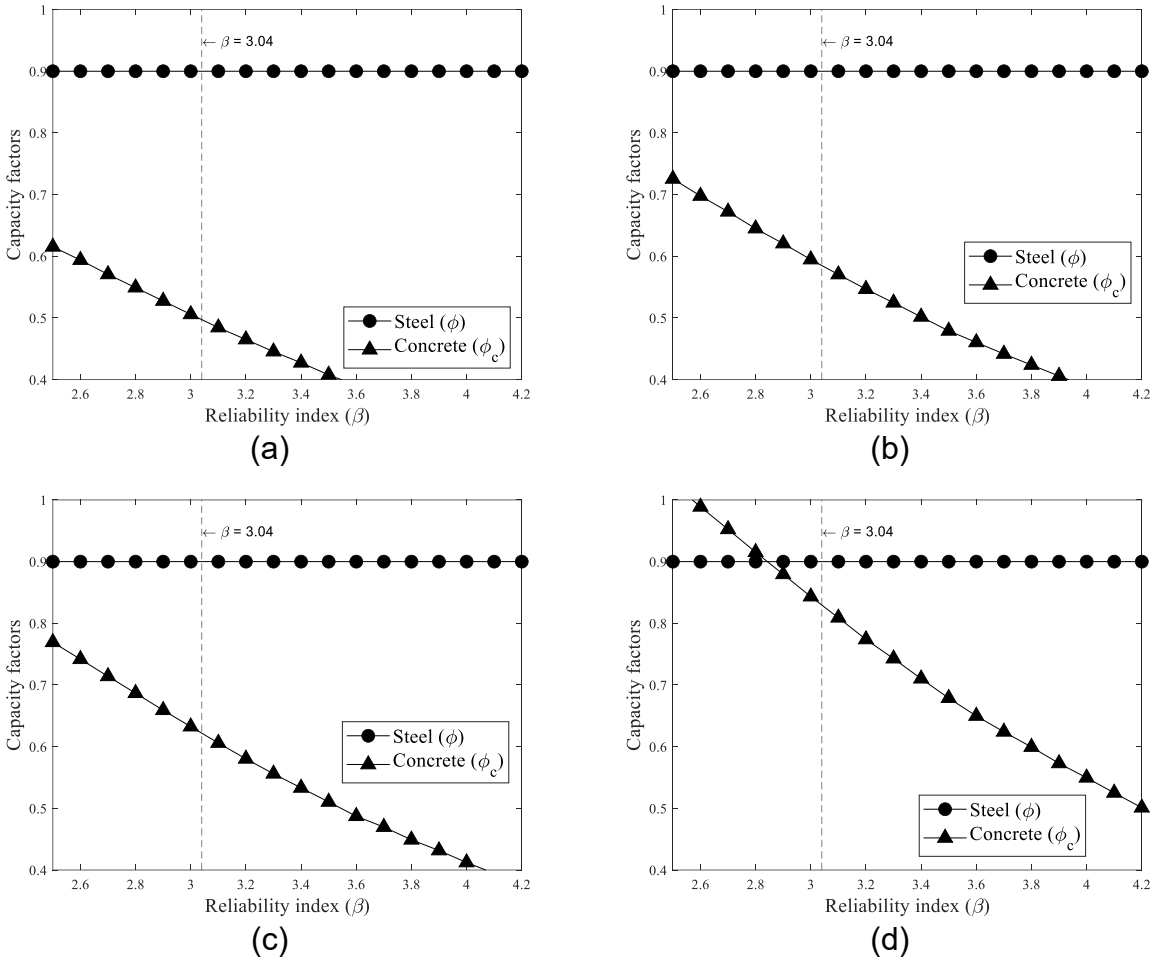

Fig. 2. Calibration of the concrete capacity factor for axial compression, with the steel capacity factor fixed at 0.9. The concrete strength reductions considered are: (a) 1.00, (b) 0.85, (c) 0.80, and (d) 0.60.

In these analyses, referring to Eqs. (5) and (8), the constant bias of the strength prediction model ($\bar{b}$) is 1.001; the modelling error (V_δ) is 0.143; the average of parametric uncertainty (V_{Rt}) is 0.083; and the overall uncertainty (V_r) is 0.164, when no additional strength reduction is applied to the concrete compressive strength. The prediction model is almost unbiased against the test results, and the modelling error has the dominant effect to the uncertainty as the same as all the other calibration practice for other composite members (Kang et al. 2018, 2021).

3.2 Composite walls under shear

For another loading condition, the data has been collected is composed of 23 specimens of composite walls under shear. The database was established based on the following references: Akiyama et al. (1991), Takeuchi et al. (1998), Ozaki et al. (2001a), Ozaki et al. (2001b). This database is used to for the modelling error estimation. The corresponding input parameters and the experimental capacity are presented in Table 2.

Table 2. Composite wall database under shear

Reference	Specimen	t_s (mm)	t_c (mm)	B (mm)	f'_c (Mpa)	f_y (Mpa)	Lateral load (kN) V_{test}
Akiyama et al. (1991)	SS050	3.2	153.6	1440	32.5	305	3250
	SS100	3.2	153.6	1440	32.5	305	3225
	SS150	3.2	153.6	1440	32.5	305	3245
Takeuchi et al. (1998)	H10T05	2.3	110.4	1775	29.7	286	2630
	H10T10	2.3	225.4	1890	32.7	286	4130
	H10T10V	2.3	225.4	1890	32.7	286	4980
	H10T15	2.3	340.4	2005	29.7	286	6700
	H07T10	2.3	225.4	1890	29.7	286	4710
	H15T10	2.3	225.4	1890	32.7	286	4000
Ozaki et al. (2001a)	BS70T05	4.5	221	1890	33.9	352.5	7370
	BS70T10	2.3	225.4	1890	33.9	389.2	5730
	BS70T14	1.6	226.8	1890	36.2	448.4	5410
	BS50T10	2.3	225.4	1890	36.2	389.2	6570
	BS85T10	2.3	225.4	1890	33.9	389.2	5450
Ozaki et al. (2001b)	S2-00NN	2.3	195.4	1200	42.2	340	3024
	S2-15NN	2.3	195.4	1200	41.6	340	3166
	S2-30NN	2.3	195.4	1200	42	340	3166
	S3-00NN	3.2	193.6	1200	41.9	351	3675
	S3-15NN	3.2	193.6	1200	41.6	351	3832
	S3-30NN	3.2	193.6	1200	40.1	351	3796
	S3-00PS	3.2	193.6	1200	41.9	351	3653
	S3-00PN	3.2	193.6	1200	39.9	351	3583
	S4-00NN	4.5	191	1200	42.8	346	4175

where V_{test} = experimentally measured shear strength of composite walls.

The shear resistance of a rectangular composite wall member is calculated as follows, which is a simplified equation based on AISC (2015) and Varma et al. (2013):

$$V_{s,Rd} = \phi(\kappa f_y A_s) \tag{16}$$

where ϕ = the unified capacity factor for walls in shear to be calibrated. κ = 1.11-5.16r; 0.60 < k < *1.0*.
where

$$\rho = \frac{A_s f_y}{A_c \sqrt{6896 f_c'}} \tag{17}$$

For the reliability analyses, the random variables are defined with means equal to the mean measured values, and their COVs are the same as in the axial compression case. Since this equation represents the steel contribution with a reduction factor and incorporates the concrete contribution through the normalised steel ratio, a single unified capacity factor is applied to the entire equation and has been calibrated accordingly.

As shown in Table 3, the constant bias is much greater than 1.0, indicating the conservatism embedded in the equation. The modelling error is dominant compared to the parametric uncertainty, and the total error has a COV of 25.1%. The corresponding unified capacity factor is calibrated as 0.77. Fig. 3 shows the calibration results across target reliability indices from 2.5 to 4.2, presenting a decreasing trend as the target reliability index increases. It also shows the calibrated capacity factor for the target reliability index of 3.04.

Table 3. Bias, uncertainties, and the unified capacity factor for composite walls under shear

	$\bar{b}$	V_δ	V_{Rt}	V_r	The unified capacity factor (φ)
Eq. (16)	1.565	0.222	0.117	0.251	0.77

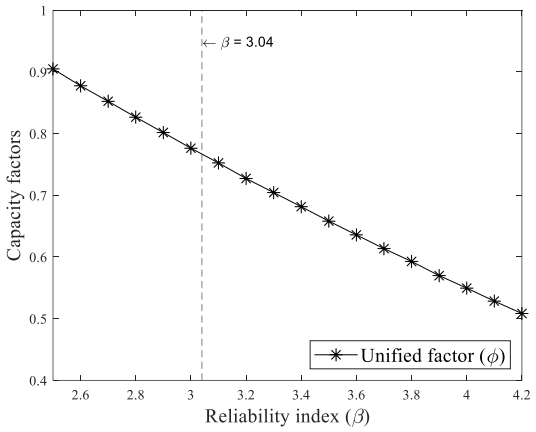

Fig. 3. Calibration of the unified capacity factor for shear

4. CONCLUSIONS

This study presents a reliability-based calibration of design capacity factors for concrete-filled steel plate composite walls to support new provisions in AS/NZS 2327. By collecting 64 axial compression tests and 23 in-plane shear tests from the literature, and by adopting reliability-based calibration procedures consistent with AS 5104, ISO 2394, and Eurocode 0 Annex D, capacity factors for composite walls under axial compression and shear have been calibrated, accounting for the effects of parametric, modelling, and statistical uncertainties on wall resistance.

For axial compression, a unified capacity factor ranging 0.64 – 0.89 satisfies the target reliability index of 3.8, with ϕ = 0.70 recommended when a concrete strength reduction factor of

0.85 is applied. When the steel factor is fixed at ϕ_s = 0.90, the corresponding concrete factors range from 0.50 to 0.83. For in-plane shear, a single unified factor of 0.77 meets the same reliability target. In all cases, modelling error dominates total variability, indicating that further refinement of prediction models offers the greatest potential for reducing design conservatism. These calibrated factors provide a consistent, cost-effective reliability level for composite wall design, aligning with existing standards for other composite members in Australian and New Zealand practice.

REFERENCES

AISC (2015), *Specification for Safety-Related Steel Structures for Nuclear Facilities, N690-12s1,* American Institute of Steel Construction, Chicago, IL.

Akiyama, H., Sekimoto, H., Fukihara, M., Nakanishi, K. and Hara, K. (1991), "A compression and shear loading test of concrete-filled steel bearing wall," *Trans. 11th Int. Conf. on Structural Mechanics in Reactor Technology (SMiRT-11),* Tokyo, Japan, Paper K04/8.

Audet, C. and Dennis, J.E. (2002), "Analysis of generalised pattern searches," *SIAM J. Optim.,* **13**(3), 889-903.

Broberg, M., Shafaei, S., Kizilarslan, E., Seo, J., Varma, A.H., Bruneau, M. and Klemencic, R. (2022), "Capacity design of coupled composite plate shear wall–concrete-filled system," *J. Struct. Eng.,* **148**(4), 04022015.

Choi, B.J. and Han, H.S. (2009), "Compressive behaviour of unstiffened steel-plate–concrete structures," *Steel Compos. Struct.,* **9**(6), 519-534.

Choi, B.J., Kang, C.K. and Park, H.Y. (2014), "Strength and behaviour of steel plate–concrete wall structures using ordinary and eco-oriented cement concrete under axial compression," *Thin-Walled Struct.,* **84**, 313-324.

Der Kiureghian, A. (2005), "First- and second-order reliability methods," *Eng. Des. Reliability Handbook,* **14**, 1-93.

European Committee for Standardization (CEN) (2002), *EN 1990: Eurocode – Basis of Structural Design,* Brussels, Belgium.

International Organization for Standardization (ISO) (1998), *ISO 2394: General Principles on Reliability for Structures,* Geneva, Switzerland.

Joint Committee on Structural Safety (JCSS) (2001), *JCSS Probabilistic Model Code,* http://www.jcss-lc.org.

Kang, W.H., Hicks, S.J., Uy, B. and Fussell, A. (2018), "Design resistance evaluation for steel and steel-concrete composite members," *J. Constr. Steel Res.,* **147**, 523-548.

Kang, W.H., Hicks, S.J., Uy, B. and Aslani, F. (2021), "Design resistance of helical seam pipe columns with limited tensile-test data," *J. Constr. Steel Res.,* **183**, 106724.

Kang, W.H., Uy, B., Tao, Z. and Hicks, S. (2015), "Design strength of concrete-filled steel columns," *Adv. Steel Constr.*, **11**(2), 165-184.

Kanchi, M., Kitano, T., Sugawara, R. and Hirakawa, K. (1996), "Experimental study on a concrete-filled steel structure. Part 2: Compressive tests (1)," *Summ. Tech. Papers Ann. Meet., Archit. Inst. Japan – Structures,* 1071-1072 (in Japanese).

Mo, J. (2022), "Behaviour and design of composite walls under axial compression," Ph.D. Thesis, The University of Sydney, Sydney, Australia.

Mo, J., Uy, B., Li, D., Thai, H.T. and Wang, Y. (2022), "Behaviour and design of composite walls under axial compression," *J. Constr. Steel Res.,* **199**, 107635.

Nocedal, J. and Wright, S. (2006), *Numerical Optimization,* Springer, New York, USA.

Ozaki, M., Akita, S., Niwa, N., Matsuo, I. and Usami, S. (2001a), "Study on steel plate-reinforced concrete bearing wall for nuclear power plants. Part 1: Shear and bending loading tests of SC walls," *Trans. 16th Int. Conf. on Structural Mechanics in Reactor Technology (SMiRT-16),* Washington, DC, Paper 1554.

Ozaki, M., Akita, S., Niwa, N., Matsuo, I. and Hara, K. (2001b), "Study on steel plate-reinforced concrete bearing wall for nuclear power plants. Part 2: Analytical method to evaluate response of SC walls," *Trans. 16th Int. Conf. on Structural Mechanics in Reactor Technology (SMiRT-16),* Washington, DC, Paper 1555.

Seo, J., Varma, A.H., Sener, K. and Ayhan, D. (2016), "Steel-plate composite walls: In-plane shear behaviour, database and design," *J. Constr. Steel Res.,* **119**, 202-215.
Standards Australia (2004), *AS 5100.6: Bridge Design – Part 6: Steel and Composite Construction,* Sydney, Australia.
Standards Australia (2017), *AS 5104: General Principles on Reliability for Structures,* Sydney, Australia.
Standards Australia/Standards New Zealand (2009), *AS/NZS 1163: Cold-Formed Structural Steel Hollow Sections,* Sydney/Wellington.
Standards Australia/Standards New Zealand (2016), *AS/NZS 3678: Structural Steel – Hot-Rolled Plates, Floorplates and Slabs,* Sydney/Wellington.
Standards Australia/Standards New Zealand (2017), *AS/NZS 2327: Composite Structures – Composite Steel-Concrete Construction in Buildings* (Incorporating Amendment 1, 2020), Sydney/Wellington.
Takeuchi, M., Narikawa, M., Matsuo, I., Hara, K. and Usami, S. (1998), "Study on a concrete-filled structure for nuclear power plants," *Nucl. Eng. Des.,* **179**(2), 209-223.
Usami, S., Hara, K., Sasaki, N., Akiyama, H., Narikawa, M. and Takeuchi, M. (1995), "Compressive loading tests on wall members," *Trans. 13th Int. Conf. on Structural Mechanics in Reactor Technology (SMiRT-13),* Porto Alegre, Brazil, Div. E, Paper 4-21-26.
Varma, A.H., Malushte, S., Sener, K. and Lai, Z. (2014), "Steel-plate composite walls for safety-related nuclear facilities: Design for in-plane force and out-of-plane moments," *Nucl. Eng. Des.,* **269**, 240-249.
Yang, Y., Liu, J. and Fan, J. (2016), "Buckling behaviour of double-skin composite walls: An experimental and modelling study," *J. Constr. Steel Res.,* **121**, 126-135.
Zhang, K., Seo, J. and Varma, A.H. (2020), "Steel-plate composite walls: Local buckling and design for axial compression," *J. Struct. Eng.,* **146**(4), 04020044.